Analytical and Bioanalytical Chemistry
https://doi.org/10.1007/s00216-020-02663-z

RESEARCH PAPER

Myoglobin-silver reduced graphene oxide nanocomposite stochastic biosensor for the determination of luteinizing hormone and follicle-stimulating hormone from saliva samples

Livia Alexandra Dinu Gugoasa[1] · Raluca-Ioana Stefan-van Staden[1] · Jacobus Frederick van Staden[1] · Maria Coros[2] · Stela Maria Pruneanu[2]

Received: 5 February 2020 / Revised: 2 April 2020 / Accepted: 15 April 2020

Abstract

A silver reduced graphene oxide (Ag-rGO) nanocomposite paste was prepared for the assay of luteinizing hormone (LH) and follicle-stimulating hormone (FSH) in children's saliva. The paste was modified with a solution of myoglobin (Myb) to form the stochastic biosensor, to improve the sensitivity of the method. The Ag-rGO powder and Myb-Ag-rGO paste were morphologically and structurally characterized by SEM, TEM and XRD measurements. For the molecular recognition of the hormones, the biosensor based on Myb-Ag-rGO reached determination limits of 8.5×10^{-3} UI L^{-1} (2.0×10^{-12} g/mL) for luteinizing hormone and 1.4×10^{-2} UI L^{-1} (1.0×10^{-12} g/mL) for follicle-stimulating hormone. The determination of both hormones in saliva samples collected from children was done with high reliability.

Keywords Luteinizing hormone · Follicle-stimulating hormone · Stochastic biosensor · Reduced graphene oxide · Silver nanoparticles

Introduction

Puberty is a complex process of development and it separates childhood from adolescence. It is characterized first by the maturation of the hypothalamic-pituitary-gonadal axis, then by the appearance of secondary sexual characteristics, followed by accelerated growth and then by the occurrence of fertility [1].

For more than 20 years, it has been observed that girls reach puberty at a much younger age, making it necessary to study the prevalence of early puberty more in depth. Puberty is considered precocious when secondary sexual characteristics occur before 8 years of age, and menstruation, in girls, occurs before the age of 9 years old [2].

Accordingly, healthcare researchers have begun to look for answers, wanting to find out why secondary sexual characteristics occur in young children of this age.

The inhibition of these hormones is higher in childhood and decreases at the beginning of puberty. In fact, in childhood, a small number of hormones produced by the gonads are able to inhibit the release of GnRH and gonadotropin secretion [3]. As puberty onset approaches, there is a progressive reduction in the sensitivity of the tonic centres receptive to sexual steroid actions. Then, a critical moment coincides with the onset of drowsiness, when gonadal hormones can no longer inhibit the neurosecretory activity of the hypothalamus. There is an increased massive release of GnRH and gonadotropins [4]: luteinizing hormone (LH) and follicle stimulating hormone (FSH), and consequent activation of the gonads leads to increased androgen circulation [5]. To be able to diagnose the precocious onset of puberty, physicians need a fast method for analysis of these hormones, easily to be

Parts of this work were presented at the XX Euroanalysis Conference in Istanbul in September 2019 and have been awarded with an ABC Best Poster Award.

Published in the topical collection *Euroanalysis XX* with guest editor Sibel A. Ozkan.

✉ Livia Alexandra Dinu Gugoasa
livia.gugoasa@yahoo.com

[1] Laboratory of Electrochemistry and PATLAB, National Institute of Research and Development for Electrochemistry and Condensed Matter, 202 Splaiul Independentei Str., 060021 Bucharest-6, Romania

[2] National Institute for Research and Development of Isotopic and Molecular Technologies, 67-103 Donat Street, 400293 Cluj-Napoca, Romania

Published online: 12 May 2020

conducted, before the critical moment mentioned above. There are only few studies available from literature about the electrochemical methods employed for the determination of LH and FSH from the same sample. The analytical methods described in literature, for the determination of LH and FSH, are mainly immunoassays, which present some drawbacks, such as expensive reagents, time-consuming analysis, limits of detection that are not applicable for children and a less stable method. To overcome these aspects, this study proposed a stochastic biosensor which was able to detect both hormones from saliva samples collected from children, being able to identify the predisposition of precocious puberty. Another important aspect of this work is the fact that for analytical application, saliva was chosen as biological sample, being a non-invasive biological matrix. The proposed stochastic biosensor was constructed from a silver reduced graphene oxide composite newly synthesized and it was modified with myoglobin, and used for the first time for the simultaneous determination of luteinizing hormone and follicle-stimulating hormone.

Reduced graphene oxide (rGO) is a derivate of graphene oxide and both materials are intensively used in the present days [6]. Due to its high conductivity, fast electron transfer rate, good mechanical strength and high surface area, rGO was used in the design of electrochemical sensors. The rGO-based materials are biocompatible and very good aspirants for biosensors with biomedical application [7].

Silver nanoparticles were chosen for the modification of graphene material to improve the graphene conductivity, to increase the active surface area and to obtain the necessary pores for the stochastic response. The last characteristic of Ag nanoparticles was also proved by the construction of a nanochannel sensing platform based on Ag nanoparticles for direct detection of a cancer biomarker in blood [8–10].

Artificial nanopores in solid membranes have proved to be a flexible tool in the analysis of single biomolecules. The use of nanopores in the design of stochastic sensors offers an interesting perspective on the detection and quantification of molecular interactions at the level of a single molecule [11]. Individual interactions between analyte molecules and pore receptor sites can be seen as modulations of the current passing through the pores.

Analyte attachment to the nanopores is random (stochastic) and reversible, and it generates specific fluctuations in the ionic current flow. This is why single nanopores inside a thin membrane have been reported as stochastic sensors and were first mentioned by Hladky and Haydon in 1970 [12]. The stochastic mechanism is based on pore conductivity and the current that flows inside and outside the pore is often measured as a function of time. The ionic current through the pore is mentioned as the open pore current. When a constant electric potential is applied in the cell, a steady-state current is generated by the exchange of ions. When the electrolyte solution contains larger biomolecules such as DNA or proteins, the analyte charged molecules are driven or translocated straight to the pore and an ionic current blockade occurs for a certain period of time [13]. One favourable aspect of stochastic mode is that two or more molecules can handle the formed pore, but at different times. That is why several analytes can be measured quantitatively and qualitatively with a single stochastic sensor. In a mixture, the signals of the different analytes are differentiated by the time each analyte blocks the channel and by the time when the analyte binds to the pore's wall [14].

The use of microsensors and biosensors for monitoring a single molecule of interest responsible for a specific type of illness is the main concern in the biomedical field. Stochastic microsensors based on diamond and carbon paste were first developed in the group of Stefan-van Staden in 2011 [15], as novel approach for organic molecule detection, with applications in the biomedical and pharmaceutical field.

Stochastic sensors based on graphene and reduced graphene oxide pastes were previously described [16–21] for fast assessment of biomolecules from biological samples. Ultrathin graphene nanopores have been designed to detect also different length DNA molecules [22, 23].

Myoglobin (Myb) is a small water-soluble hemoprotein found in the muscles. It has only one polypeptide chain, which contains an iron heme centre, and it was used as the biocompatible component added in the novel synthesized Ag-rGO nanocomposite paste. Myb can strongly adhere on the surface of Ag-rGO nanocomposite to form the modified stochastic paste biosensor. The activity centre of Myb (the Fe^{3+} ion from the heme part of the protein) is so deeply hidden inside the protein shells that direct electron transfer will not influence the determination of the hormones in solution [24]. The Myb biomolecule can bind LH and FSH in the pores of the modified graphene paste.

This paper proposed the immobilization of myoglobin in the newly synthesized silver reduced graphene oxide material for the design of a stochastic biosensor used for the molecular determination of luteinizing hormone and follicle-stimulating hormone from saliva samples.

Experimental

Materials and reagents

Luteinizing hormone (LH), follicle-stimulating hormone, monosodium phosphate, disodium phosphate, potassium chloride and paraffin oil were purchased from Sigma-Aldrich (Milwaukee, USA) (d_4^{20}, 0.86 $g \times cm^{-1}$). Graphite rods (6 mm diameter, 99.9995% purity) and silver nitrate ($AgNO_3$) were purchased from Alfa Aesar (Germany); sulfuric and nitric acids from Reactivul Bucuresti. Distilled water

was obtained using a Millipore direct-Q3 system (Molsheim, France) and added to prepare all solutions. Monosodium and disodium phosphate were used to prepare phosphate buffer saline solution at pH 7.4. LH stock solution (14.0×10^3 UI L^{-1}) was reconstituted following the manufacturer's information sheet from 2.0 μg in 1 mL of PBS at pH 7.4. FSH stock solution (85.0×10^3 UI L^{-1}) was reconstituted according to the manufacturer's information sheet from 10.0 μg in 1 mL of PBS at pH 7.4. Serial dilution technique was used for the preparation of different concentrations for LH solutions (1.4×10^3 UI L^{-1}–1.4×10^{-4} UI L^{-1}), and FSH (8.5×10^4 UI L^{-1}–8.5×10^{-4} UI L^{-1}) buffered with phosphate buffer solution of pH = 7.4. When not in use, all solutions were stored in the fridge, at 4–8 °C.

Apparatus and methods

All electrochemical measurements were performed with a potentionstat/galvanostat AUTOLAB/PGSTAT 302 (Methrom, Utrecht, The Netherland) connected to a personal PC, where a GPES software was used to record the measurements and process the result data. All experimental measurements were performed at room temperature.

Transmission electron microscopy (TEM), scanning electron microscopy (SEM) and scanning transmission electron microscopy (STEM) with energy-dispersive X-ray (EDX) spectroscopy technique were used to investigate the morphology and the elemental distribution of atoms (C, Ag, O) (SU-8230 STEM system, Hitachi, Japan) within the Ag-rGO composite.

For structural investigation of the Ag-rGO and Myb-Ag-rGO samples, the X-ray powder diffraction (XRD) technique was employed. Each sample pattern was recorded with DIFFRAC plus XRD Commander a Bruker D8 advance diffractometer (40 kV, 0.5 mA) equipped with a LYNXEXE detector (0.02° s^{-1} scan speed; $\lambda = 1.5406$ Å—$CuK_{\alpha 1}$ radiation). Before plotting the experimental results, the spectrum background was corrected using WinPLOTR software.

For Ag-rGO sample lyophilization, a Christ alpha 1-4 LSC freeze dryer was used.

Preparation of Ag-rGO nanocomposite

The Ag-rGO nanocomposite was prepared by electrochemical exfoliation of graphite rod using pulses of current [25]. The exfoliation was performed in acidic solution consisting of a mixture of H_2SO_4:HNO_3 (3:1 ratio; 0.5 M each; 100 mL total volume). The current pulse duration was set at 2.5 s and the pause between two pulses was set at 0.8 s. A low voltage (4.5 V) was applied on the electrodes for 2 h. Next day, the exfoliated material was washed with bi-distilled water, filtered, sonicated and dried by lyophilization. Ag-rGO was prepared by thermal reduction of starting material obtained by electrochemical exfoliation as was described above. One hundred fifty milligrammes exfoliated material, 0.785 mL H_2O and 7 mg $AgNO_3$ were mixed together and left to dry at room temperature. The thermal reduction took place at 250 °C (15 min) in an Ar-H_2 atmosphere. The sample was following denoted as Ag-rGO.

The design of the stochastic paste microsensor and biosensor

The synthesized Ag-rGO was mixed with paraffin oil until homogenous paste was obtained. The paste was divided in two parts: one part was modified with 5 μL of myoglobin (1.0 mg/mL) and the other one was used as it was. Each paste was placed in a plastic micropipette tip (300 nm internal diameter). A silver wire was inserted into the plastic tip to create the electrical contact (0.3 mm in diameter) between the external circuit and the conductive paste. An Ag/AgCl microsensor and Pt wire served as reference and auxiliary microelectrodes in the electrochemical cell. Every morning and before each measurement, the sensors were cleaned with deionized water. When not in use, they were stored in the fridge (2–8 °C).

Samples

Ten saliva samples were collected from children and teenagers in the same day before breakfast (ethics committee approval no. 158/2018, awarded by the University of Medicine and Pharmacy "Carol Davila" in Bucharest), being more than 10 h since dinner, last beverage and teeth cleansing. Saliva was acquired from each patient after 2 successive mouth rinses with water. Less than 3 mL of saliva spit was taken from each child and after elimination of any food residue by centrifugation, each saliva sample was divided in small aliquots (1 mL) and stored in a very low–temperature freezer (−80 °C). Informed consent was obtained from all parents or legal tutors of the patients. The samples were analysed as received using the stochastic microsensors, for the molecular recognition of both LH and FSH.

Results and discussion

Morphological and structural characterization of Ag-rGO nanocomposite

The modification with silver of the reduced graphene material was needed because by using only reduced graphene oxide material, no response was obtained for the stochastic sensor. The TEM/SEM images of Ag-rGO nanocomposite are presented in Fig. 1a and b, respectively.

One can notice the presence of irregular and wrinkled graphene flakes with size of hundred of nanometres. The silver

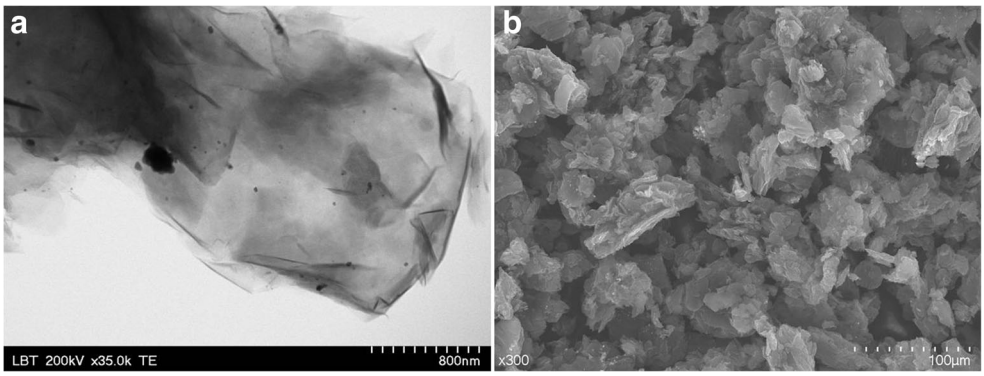

Fig. 1 **a**) TEM - showing the presence of irregular and wrinkled graphene flakes and the dark spots represent the silver nanoparticles, uniformly distributed on the graphene sheet; and **b**) SEM image of Ag-rGO sample - showing the material porosity; scale bar: 800 nm (**a**) and 100 µm (**b**)

nanoparticles (dark spots in TEM image—Fig. 1a) are relatively uniform distributed on the graphene surface. In addition, the TEM image shows the co-existence of thin and transparent flakes made of few-layer graphene (FLG) and thicker flakes representing multi-layer graphene (MLG). The material porosity can be clearly seen in the representative SEM image (Fig. 1b). The elemental distribution of carbon, oxygen and silver on the graphene surface was revealed by STEM-EDX mapping (Fig. 2). The spectrum in Fig. 2b illustrates the presence of carbon and silver, with a small percentage of oxygen (3.9 wt.%) originating from the graphene oxide sheet.

In Fig. 3, the XRD patterns of the electrochemically exfoliated sample are presented, before and after silver nanoparticles deposition, as well as after mixing the sample with myoglobin and paraffin oil. Immediately after exfoliation, the sample contains a large amount of graphene oxide—GO ($2\theta = 13.8°$) along with significant amounts of FLG and MLG flakes (Fig. 3a). The thermal reduction in the presence of silver nitrate changed the pattern (Fig. 3b). Consequently, the GO peak almost disappeared while the attachment of silver nanoparticles to graphene surface is proved by the presence of several characteristic peaks of silver. Significant changes can be seen after myoglobin and paraffin oil were mixed with Ag-rGO sample, in order to obtain the paste electrode (Fig. 3c). The crystallite size value (*D*) was calculated from the full width at half maximum (FWHM) using the Debye-Scherrer equation:

$$D = \frac{0.9 \times \lambda}{\beta \times \cos\theta} \tag{1}$$

where λ is the X-ray wavelength, β is FWHM expressed in radians, and θ is half the diffraction angle of the peak (in degrees) corresponding to interlayer distance, *d*. The *interlayer distance* value was found with Bragg equation ($d = \lambda/2 \sin \theta$), while the average number of layers, *n*, was calculated from the relation $n = D/d$ [26].

The amount of each type of graphene (GO; FLG and MLG) within the samples was determined from the XRD pattern by dividing the area of each peak to the total area of the diffractogram. The peak around 26° is large and asymmetric and it was separated in two theoretical Gaussian peaks which represent the FLG and MLG flakes (Fig. 3). The starting material consists of graphene oxide (37%), FLG (44%) and MLG (19%). The interlayer

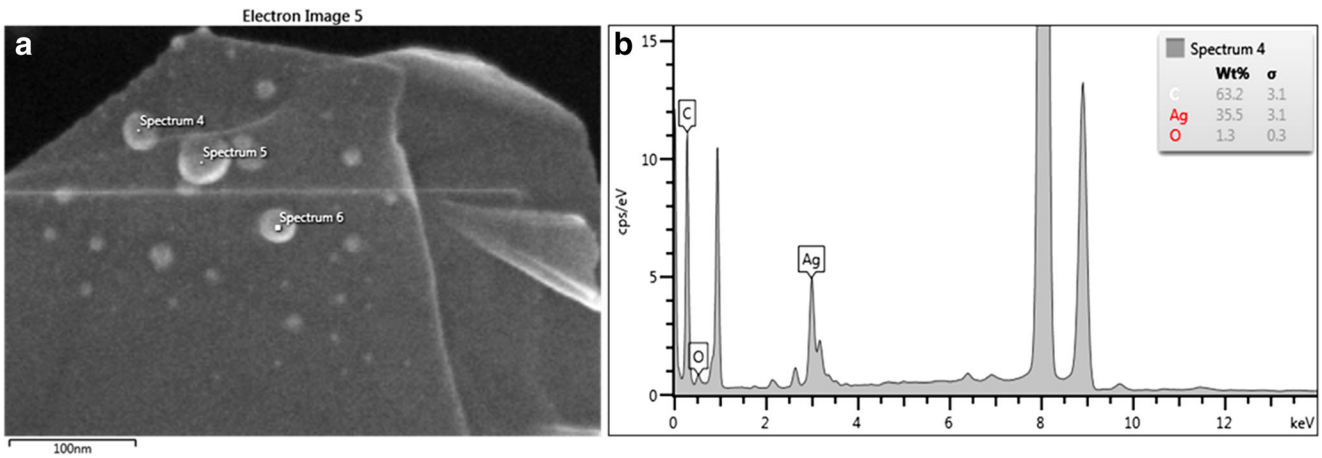

Fig. 2 Elemental distribution of C, O and Ag in Ag-rGO sample

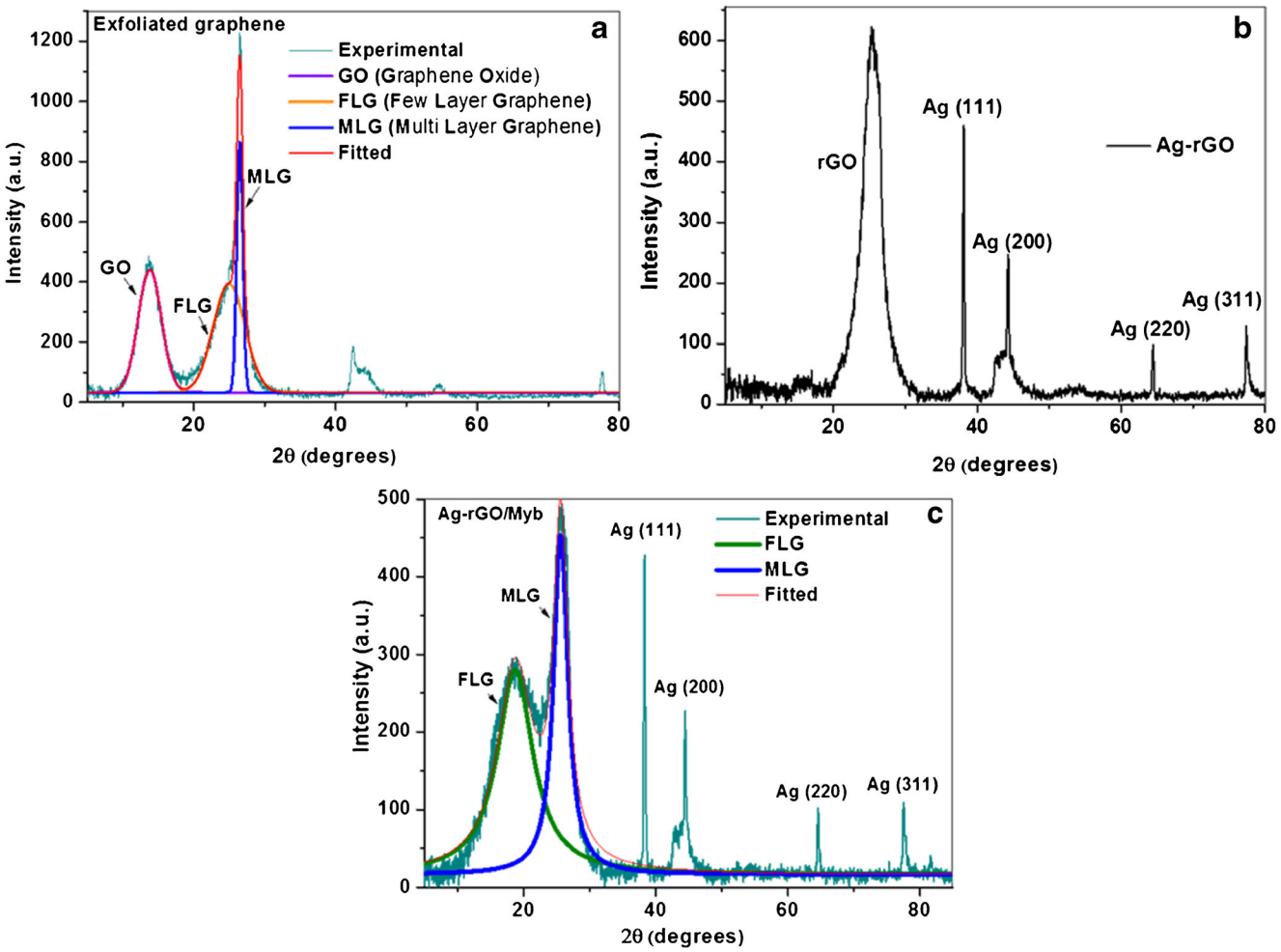

Fig. 3 X-ray diffraction pattern of the electrochemically exfoliated sample before (**a**) and after (**b**) silver nanoparticles (Ag) deposition, obtaining the silver-reduced graphene oxide (Ag-rGO) (**c**) after myoglobin (Myb) and paraffin oil incorporation, obtaining the silver-reduced graphene oxide modified with myoglobin (Ag-rGO/Myb)

distance varies between 0.641 nm (for GO) and 0.356 nm (for FLG). In the case of MLG, the interlayer distance is around 0.336 nm.

The thermal reduction proved to be very efficient. Thus, after silver nanoparticle's deposition, the material presented a more uniform structure, the Ag-rGO sample consisting of 8 layers of graphene with an interlayer distance of 0.35 nm (Fig. 3b). The diffraction lines from 38°, 44.2°, 64.4° and 77.4° were attributed to (111), (200), (220) and (311) reflection of silver. Their intensity suggests that a large amount of silver nanoparticles was attached to the graphene surface, being in good agreement with TEM/SEM images. The mean crystallite size of AgNPs determined with the Scherrer equation was around 37 nm. After myoglobin and paraffin oil incorporation, the sample consisted of a mixture of 3 layers (60%) and 9 layers of graphene (40%) with an interlayer distance of 0.47 nm and 0.35 nm, respectively (Fig. 3c).

The stochastic mode

The chronoamperometric technique was used for the measurements of the t_{on} and t_{off} parameters. The t_{off} value represents the signature of the analyte, while the t_{on} value represents the quantitative parameter. The stochastic mode was used for both qualitative and quantitative assays of the LH and FSH from real samples. The measurements were carried out at a constant potential of 0.125 V, in 360 s for calibration measurements of each analyte and for the saliva sample measurements. Based on each hormone's unique t_{off} value determined from the calibration curve, it was possible to identify them in the diagram recorded for the biological saliva samples, and further to measure the parameter t_{on} value. The unknown levels of the hormones were measured using the equation of calibration $1/t_{on} = f(\text{conc}_{\text{hormone}})$ [14] recorded for each stochastic microsensor. All measurements were carried out at room temperature.

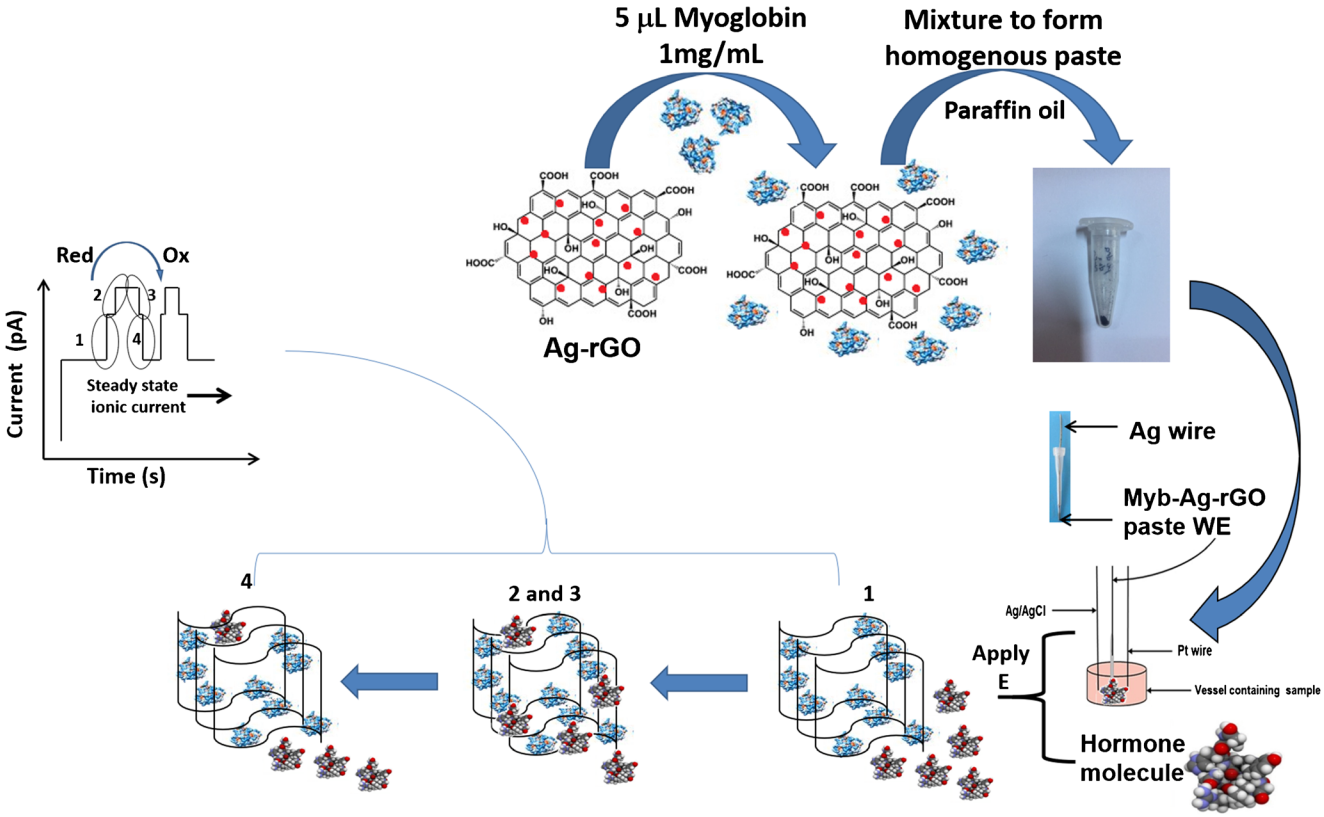

Fig. 4 Schematic representation of the current development for stochastic sensors and the construction steps of the stochastic biosensor and the reaction process of the interaction of silver-reduced graphene oxide modified with myoglobin (Myb-Ag-rGO) based biosensor with the two hormones, LH and FSH. The current fluctuations are given by the (1) increasing ionic current due to the flow of molecules towards the solution-electrode interface, (1–2) followed by a blockage of the ionic current for a certain period of time (t_{off}), given by the entrance of the hormone in the pore; (2) the interaction of the hormone with the pore, described by an increase in current, followed by (2–3) a constant current intensity recorded for a certain period of time (t_{on}) and (3) the decrease in current due to the charge change of the molecule; (3–4) the moment when the molecule leaves the pore and (4) the return to the steady state ionic current. The electrochemical cell (down right) is formed from the working electrode, the silver-silver chloride (Ag/AgCl) as reference electrode and the platinum wire (Pt wire) as counter electrode

The construction of the stochastic biosensor based on the Myb-Ag-rGO paste is represented in Fig. 4. The interaction of Myb with LH and FSH is also represented in Fig. 4. When applying a constant potential to the proposed biosensor in a 0.1 mol L^{-1} phosphate buffer saline solution of pH 7.4, a steady-state current is recorded. When adding different concentrations of hormones to the PBS solution, the current fluctuates as shown in Fig. 4. Each hormone molecule interacts with the pores formed by the Myb molecules on top of the Ag-rGO material. When the potential is applied on the working electrode, the hormone's molecules are flowing towards the solution-electrode interface (1). Each hormone molecule interacts with the pore through the amino acid residues that both the hormone and myoglobin contain. During this interaction, the hormone molecule enters the pore gradually until it fills almost completely the pore cavity formed in the Myb-Ag-rGO material. So, the ionic flux is blocked for a certain period of time (t_{off}) until the oxidation process takes place (2). The oxidized form of the hormone leaves the cavity gradually. This can be observed when the current intensity decreases and returns to the steady state (3 and 4), waiting for another reduced hormone molecule to interact with the pore.

Influence of pH

The composition and type of the buffer solution are other parameters affecting the interaction between the molecules and the graphene nanocomposite. Alkaline pH values minimize the interaction with the surface, leading to faster denaturation of the hormones [27]. The electrochemical cell contains 0.1 mol L^{-1} phosphate buffer saline solution, as supporting electrolyte, so Na^+ ions and phosphate ions will provide the ionic current flow.

The pH value is a very important electrochemical parameter due to the pKa values of the molecules or isoelectric point of the proteins. Adapting the pH value to a neutral value was used to avoid subunit dissociation of LH and FSH and provide accurate analysis of both hormones.

Furthermore, pH 7.4 is the physiologic pH value found in the body, so for a precise measurement of the biological

samples, such as saliva or serum, pH 7.4 phosphate buffer saline solution was used to prepare LH and FSH standard solutions.

Response characteristics of stochastic microsensors

The response characteristics of the proposed stochastic microsensors for the evaluation of FSH and LH standard solutions are summarized in Table 1. The myoglobin modification on the Ag-rGO paste (Figs. 5c and 6c) showed a better response than the Ag-rGO paste microsensor (Figs. 5a and 6a) towards screening of FSH and LH standard solutions. The determination limits using the stochastic biosensor based on the Myb-Ag-rGO paste for FSH (1.4×10^{-2} UI L^{-1}) and LH (8.5×10^{-3} UI L^{-1}) were lower than those obtained from the stochastic microsensor based on Ag-rGO paste: FSH (1.4×10^{-1} UI L^{-1}) and LH (8.5×10^{-2} UI L^{-1}). As it can be seen from Table 2, the stochastic method proposed reached the lowest determination limit for both hormones, LH and FSH.

The t_{off} values were calculated as periods of time when the current drops and each hormone extracted from the solution binds to the pore wall. The stochastic biosensor based on the Myb-Ag-rGO paste presented the highest sensitivities (4.0×10^{-4} s^{-1}/UI L^{-1} for FSH calibration and 8.8×10^{-5} s^{-1}/UI L^{-1} for LH) (Figs. 5d and 6d), making it a good choice for fast screening of both hormones in saliva samples.

For the calibration of both hormones, the stochastic biosensor based on the Myb-Ag-rGO paste covered a wider concentration range than the stochastic microsensor based on Ag-rGO paste. In Figs. 5b and 6b, the calibration curves for both hormones were presented, and in the inset, the equation of calibration for each sensor for the determination of each hormone is shown, with very good correlation coefficients.

Selectivity

Stochastic detection is very sensitive and also quite selective. Stochastic sensors do not need to contain a selective element, since each analyte has a specific signature (t_{off}). Each biological molecule is unique and the molecular recognition is based on the size of the biological molecule, geometry of the biological molecule and the folded or unfolded form of the biological molecule [14].

The selectivity of the pore during the on and off processes of individual molecules is due to the high time resolution and high current sensitivity of the technique, with no prior information about the molecule sequence required. Moreover, this proposed method can be used to select small components of complex samples [33].

Due to this aspect, the confusions that generally arise in all other analytical techniques by which the signal of some similar structures overlaps in the analysis of the analyte of interest are eliminated. The different t_{off} values for each hormone

Table 1 Response characteristics of the stochastic microsensor and biosensor for determination of FSH and LH

Stochastic sensor based on	Calibration equation* and correlation coefficient (r)	Linear concentration range (UI/L)	t_{off} (s)	Sensitivity (s^{-1}/UI L^{-1})	Limit of determination (UI/L)
FSH					
Ag-rGO	$1/t_{on} = 0.026 (\pm 5.8 \times 10^{-4}) + 9.8 \times 10^{-4} (\pm 7.9 \times 10^{-5}) \times C_{FSH}$ $r = 0.9996$	1.4×10^{-1}–1.4×10^{1}	2.6	1.0×10^{-3}	1.4×10^{-1}
Myb-Ag-rGO	$1/t_{on} = 0.023 (\pm 4.1 \times 10^{-4}) + 4.0 \times 10^{-4} (\pm 6.5 \times 10^{-6}) \times C_{FSH}$ $r = 0.9995$	1.4×10^{-2}–1.4×10^{2}	2.6	4.0×10^{-4}	1.4×10^{-2}
LH					
Ag-rGO	$1/t_{on} = 0.042 (\pm 9.9 \times 10^{-4}) + 2.0 \times 10^{-3} (\pm 2.1 \times 10^{-4}) \times C_{LH}$ $r = 0.9996$	8.5×10^{-2}–8.5×10^{0}	1.9	2.0×10^{-3}	8.5×10^{-2}
Myb-Ag-rGO	$1/t_{on} = 0.023 (\pm 6.5 \times 10^{-4}) + 8.8 \times 10^{-5} (\pm 1.8 \times 10^{-6}) \times C_{LH}$ $r = 0.9996$	8.5×10^{-3}–8.5×10^{2}	1.9	8.8×10^{-5}	8.5×10^{-3}

*C_{FSH} = UI/L; C_{LH} = UI/L

using the stochastic microsensor based on Ag-rGO paste and the stochastic biosensor based on Myb-Ag-rGO paste are presented in Table 3 and they make possible the identification of both hormones in a mixture, or in a biological sample.

It follows from Table 3 that the binding times (t_{off} values) of each hormone are similar for both proposed stochastic sensors, due to the size and geometry of each hormone, which remains the same before entering the pores of both materials.

Analytical applications

The saliva samples for this study were collected from obese children patients with ages between 7 and 13 years old, 4 girls and 5 boys, and from a teenager girl patient.

The maximum values of the concentration range for healthy and normal weight children patients were 11.1 UI L^{-1} for FSH and 11.9 UI L^{-1} for girls under 14 years old and 4.6 UI L^{-1} for FSH and 7.8 UI L^{-1} for boys under 14 years old (Synevo Medical Laboratories standards). The average levels of hormones in saliva samples measured using the proposed method were higher than the normal levels and they were correlated with high body mass index (BMI) of the children patients (above 97th BMI percentile), knowing that obesity is a contributing factor for precocious puberty. So, all obese children patients showed high salivary levels of LH and FSH.

The stochastic microsensor based on Ag-rGO without Myb covers a smaller linear range of concentrations for both hormones: from 0.14 UI L^{-1} until 14 UI L^{-1} for FSH and from 0.085 UI L^{-1} until 8.5 UI L^{-1} for LH. Higher amounts like in the case of the samples involved in this study (from obese children) cannot be measured using the stochastic microsensor based on Ag-rGO paste, only using the stochastic biosensor based on the Myb-Ag-rGO paste (Table 4). The stochastic

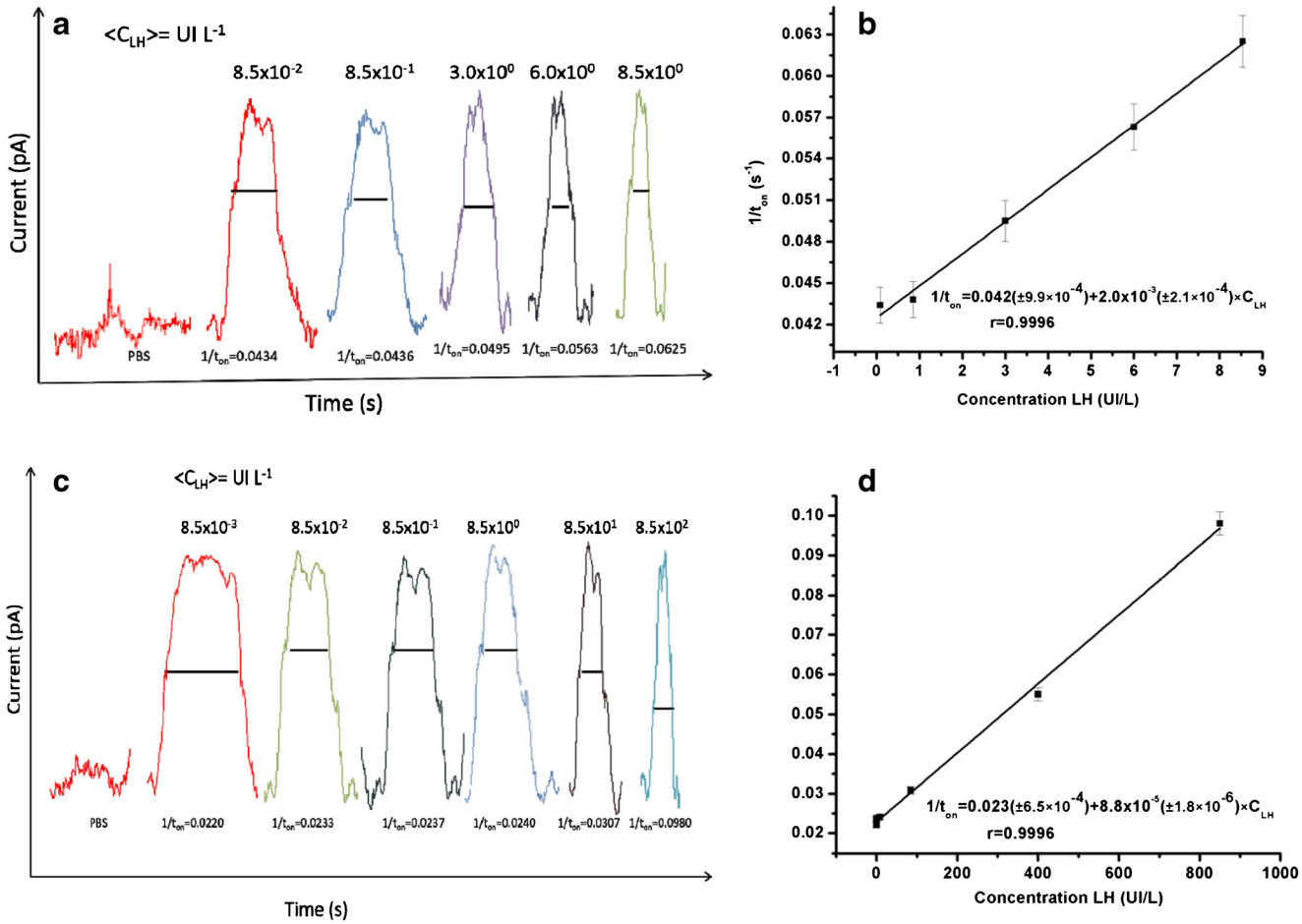

Fig. 5 Chronoamperometric peaks corresponding to qualitative parameter, $t_{off} = 1.9$ and increasing quantitative parameter, $1/t_{on}$ values extracted from the measurements recorded using (**a**) the Ag-rGO paste microsensor and (**c**) the Myb-Ag-rGO paste biosensor in PBS 0.1 mol L^{-1} containing also different concentrations of LH. Calibration curves for LH determination using (**b**) the Ag-rGO paste microsensor and (**d**) Myb-Ag-rGO paste biosensor

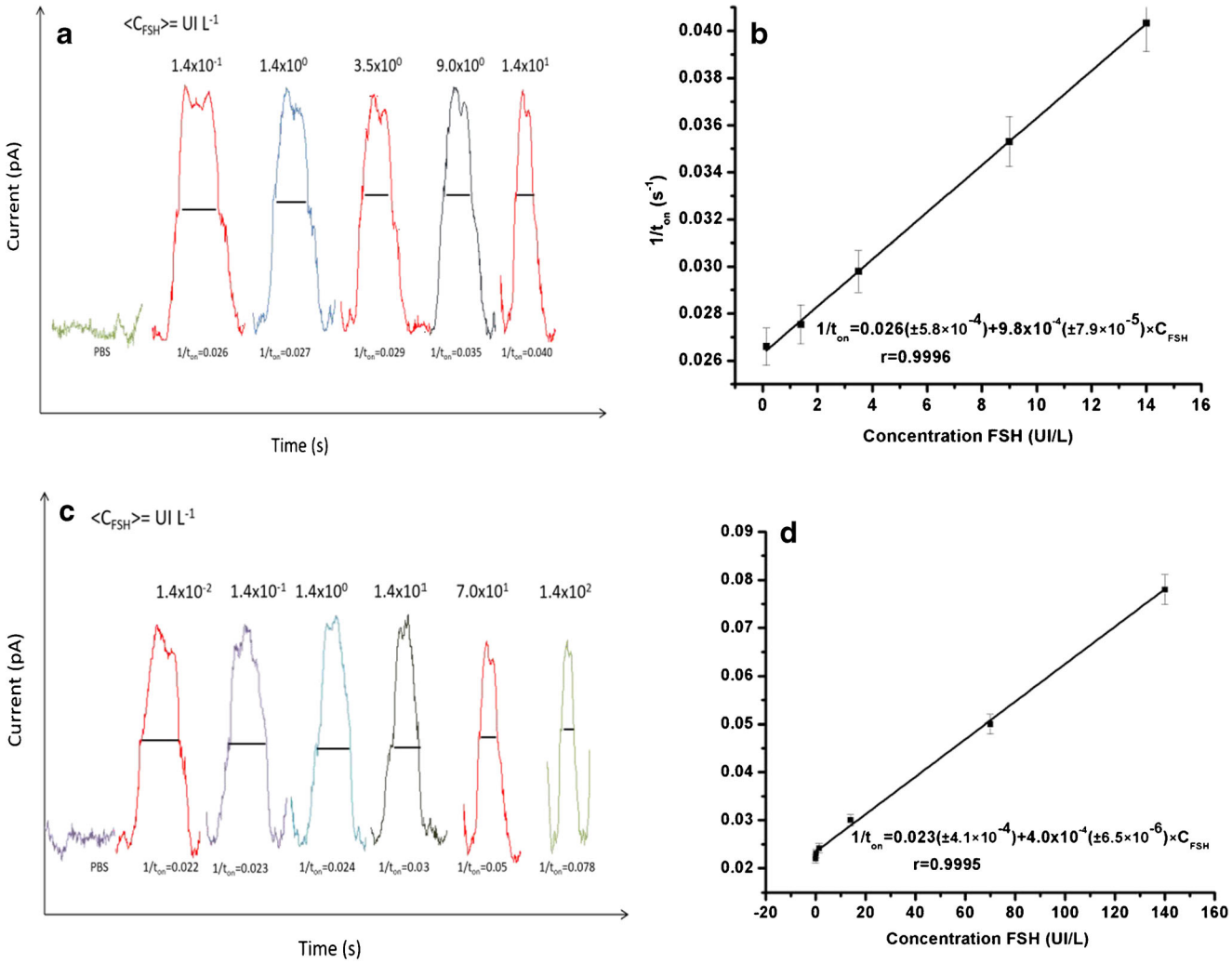

Fig. 6 Chronoamperometric peaks corresponding to qualitative parameter $t_{off} = 2.6$ and increasing quantitative parameter, $1/t_{on}$ values extracted from the measurements recorded using (**a**) the Ag-rGO microsensor and (**c**) the Myb-Ag-rGO paste biosensor in PBS 0.1 mol L^{-1} containing also different concentrations of FSH. Calibration curves for FSH determination using (**b**) the Ag-rGO paste microsensor and (**d**) the Myb-Ag-rGO paste biosensor

Table 2 Analytical methods for determination of LH and FSH

Method	Limit of determination (g/mL)	Samples	Reference
LH			
Enzyme immunoassay	2.5×10^{-12}	Chicken plasma	[28]
Immunosensor	2.5×10^{-10}	Serum sample	[29]
SPR immunoassay	1.0×10^{-9}	Serum sample	[30]
Sandwich immunoenzymometric assays	6.5×10^{-11}	Urine sample	[31]
Enzyme-linked immunosorbent assay	2.4×10^{-9}	Tilapia fish	[32]
Myb-Ag-rGO stochastic microsensor	2.0×10^{-12}	Children saliva samples	This work
FSH			
Immunosensor	2.4×10^{-10}	Serum sample	[29]
SPR immunoassay	1.0×10^{-9}	Serum sample	[30]
Sandwich immunoenzymometric assays	2.0×10^{-10}	Urine sample	[31]
Enzyme-linked immunosorbent assay	1.5×10^{-9}	Tilapia fish	[32]
Myb-Ag-rGO stochastic microsensor	1.0×10^{-12}	Children saliva samples	This work

Table 3 Qualitative signature based on t_{off} values for FSH and LH using Ag-rGO paste microsensor and Myb-Ag-rGO paste biosensor

Stochastic sensor based on	Selective parameter t_{off} (s) for	
	FSH	LH
Ag-rGO	2.6	1.9
Myb-Ag-rGO	2.6	1.9

microsensor based on Ag-rGO paste can be used for normal weight children patients (Fig. 7a), without any other reproductive disorder (which can provoke an increase in hormonal level even for normal weight patients), just for a routine checkup.

The amounts of hormones found using the stochastic biosensor based on Myb-Ag-rGO in the saliva samples collected from obese children were higher than the normal levels for healthy children (Table 4), proving the correlation between childhood obesity and the onset of precocious puberty. Figure 7b shows the stochastic diagram for the determination of LH and FSH from saliva sample using the stochastic biosensor based on the Myb-Ag-rGO.

Also, one can say that the stochastic biosensor based on the Myb-Ag-rGO paste may be able to determine low levels of LH and FSH, due to the fact that it reaches lower determination limits for LH and FSH, than the standard method detection limit (0.1 UI L^{-1}, Synevo Medical Laboratories standards). Low levels are present in infants, toddlers and children under age of 7 years and are not detectable with the standard method, but knowing the concentration of these hormones is important to prevent the possible onset of precocious puberty.

Conclusions

In this paper, two stochastic microsensors based on Ag-rGO and Myb-Ag-rGO pastes respectively were evaluated for the simultaneous determination of LH and FSH from saliva samples. The Myb modification of the Ag-rGO paste showed improvements in the determination of each hormone such as the following: the concentration ranges were wider for the determination of FSH 1.4×10^{-2} UI L^{-1}–1.4×10^{2} UI L^{-1}, instead of 1.4×10^{-1} UI L^{-1}–1.4×10^{1} UI L^{-1}, and for the determination of LH 8.5×10^{-3} UI L^{-1}–8.5×10^{2} UI L^{-1}, instead of 8.5×10^{-2} UI L^{-1}–8.5 UI L^{-1}; the limits of determination were lower: 1.4×10^{-2} UI L^{-1} for FSH and 8.5×10^{-3} UI L^{-1} for LH; also the sensitivities were higher: for FSH determination 4.0×10^{-4} s^{-1}/UI L^{-1}, instead of 1.0×10^{-3} s^{-1}/UI L^{-1}, and for LH: 8.8×10^{-5} s^{-1}/UI L^{-1}, instead of 2.0×10^{-3} s^{-1}/UI L^{-1}. The Myb biomolecule can easier bind LH and FSH, which are larger molecules, in the pores of the modified graphene paste. Using the proposed stochastic biosensor based on Myb-Ag-rGO, the salivary hormonal levels of LH and FSH were determined and correlated with high body mass index (BMI) of the children patients (above 97th BMI percentile).

Table 4 FSH and LH levels in saliva sample using the stochastic biosensor based on Myb-Ag-rGO paste

Age (years)	Sex	Weight profile	Stochastic paste biosensor based on Myb-Ag-rGO		Standard method (ECLIA[Z])	
			Amount found (UI/L)		Normal ranges (UI/L) of (regarding age and gender)	
			FSH	LH	FSH*	LH**
7	F	Obese	12.9	2.8	0.3–11.1	0.1–1.4
11	M	Obese	8.5	57.4	0.4–4.6	0.1–7.8
16	F	Obese	24.4	147.2	1.7–21.5	1.0–95.6
11	M	Obese	10.9	60.9	0.4–4.6	0.1–7.8
14	M	Obese	21.3	90.1	1.5–12.9	1.3–9.8
7	M	Obese	9.1	2.2	0.4–3.8	0.1–1.4
13	M	Obese	5.3	66.8	0.4–4.6	0.1–7.8
11	F	Normal weight	7.1	19.6	2.1–11.1	0.0–11.9
11	F	Normal weight	10.3	8.6	2.1–11.1	0.0–11.9
14	F	Normal weight	15.0	10.5	1.7–21.5	1.0–95.6

[Z] Electrochemiluminescence immunoassay

*Normal level range of FSH regarding age and gender from Synevo Medical Laboratories standards

**Normal level range of LH regarding age and gender from Synevo Medical Laboratories standards

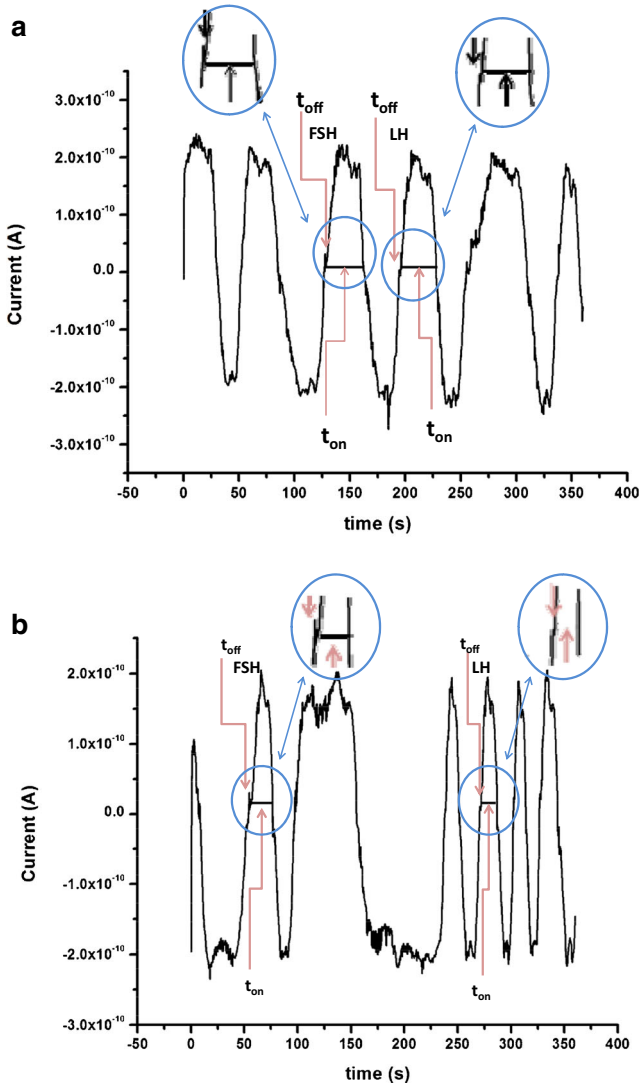

Fig. 7 Example of the stochastic diagram recorded for the assay of FSH and LH in saliva samples using (**a**) the Ag-rGO paste stochastic microsensor and (**b**) the Myb-Ag-rGO paste stochastic biosensor. The t_{off} is the qualitative parameter having different value for each of the two hormonoes (t_{off}=1.9 for LH and t_{off}=2.6 for FSH)and t_{on} is the quantitative parameter

Acknowledgments The authors are grateful to Dr. Lucian-Barbu Tudoran for performing TEM/SEM measurements and to PhD student Alexandru Turza for recording the XRD measurements.

Funding information This work was financially supported by a grant of the Ministry of Research and Innovation, CNCS-UEFISCDI, project number PN-III-P1-1.1-PD-2016-0190, within PNCDI III. TEM/SEM measurements were partially supported through the infrastructure obtained in the Project: Research Center and Advanced Technologies for Alternative Energies - CETATEA - 623/11.03.2014.

Compliance with ethical standards

Informed consent was obtained from all parents or legal tutors of the patients.

Conflict of interest The authors declare that they have no conflicts of interest.

References

1. Kakarla N, Bradshaw K. Disorders of pubertal development precocious puberty. Semin Reprod Med. 2003;21:339–51.
2. Kaplowitz P. Diagnosing children with signs of early puberty: knowing when to test and when to just monitor. Expert Rev Endocrinol Metab. 2016;11:297–9.
3. Dunkel L, Alfthan H, Stenman UH, Selstam G, Rosberg S, Albertsson-Wikland K. Development changes in 24-hour profiles of luteinizing hormone and follicle-stimulating hormone from prepuberty to midstages of puberty in boys. J Clin Endocrinol Metab. 1992;74:890–7.
4. Yan F, Zhang M, Li J. Solution-gated graphene transistors for chemical and biological sensors. Adv Healthc Mater. 2014;3:313–31.
5. Wu JF, Xu MQ, Zhao GC. Graphene-based modified electrode for the direct electron transfer of cytochrome c and biosensing. Electrochem Commun. 2010;12:175–7.
6. Tashkhourian J, Nezhad MRH, Khodavesi J, Javadi S. Silver nanoparticles modified carbon nanotube paste electrode for simultaneous determination of dopamine and ascorbic acid. J Electroanal Chem. 2009;633:85–91.
7. Ojani R, Safshekan S, Raoof JB. Silver nanoparticle decorated poly(2-aminodiphenylamine) modified carbon paste electrode as a simple and efficient Electrocatalyst for oxidation of formaldehyde. Chin J Catal. 2014;35:1565–70.
8. de la Escosura-Muniz A, Mercoki A. A nanochannel/nanoparticle-based filtering and sensing platform for direct detection of a cancer biomarker in blood. Small. 2011;7:675–82.
9. Seidlitz HK, Schneckenburger H, Stettmeier K. Time-resolved polarization measurements of porphyrin fluorescence in solution and in single cells. J Photochem Photobiol B. 1990;5:391–400.
10. Hladky SB, Haydon DA. Discreteness of conductance change in bimolecular lipid membranes in the presence of certain antibiotics. Nature. 1970;225:451–3.
11. Miles BN, Ivanov AP, Wilson KA, Dogan F, Japrung D, Edel JB. Single molecule sensing with solid-state nanopores. Chem Soc Rev. 2013;42:15–28.
12. Bayley H, Cremer PS. Stochastic sensors inspired by biology. Nature. 2001;413:226–30.
13. Stefan-van Staden RI, van Staden JF, Balasoiu SC. Disposable stochastic dot sensors for the assay of ascorbic acid in pharmaceutical samples, beverages, and biological fluids. Anal Lett. 2011;44:2280–6.
14. Stefan-van Staden RI, Gugoasa LA, Biris AR. Pattern recognition of monocyte chemoattractant protein-1 (MCP-1) in whole blood samples using new platforms based on nanostructured materials. Nanoscale. 2015;7:14848–53.
15. Gugoasa LA, Stefan-van Staden RI, Dima A, Visan CA, Streinu-Cercel A, Biris A, et al. Fast screening of biological fluids for cytokines and adipokines using stochastic sensing. Microelectron Eng. 2015;148:64–9.
16. Stefan-van Staden RI, Gugoasa LA, Socaci C, Biris AR. New nanocomposites-graphene pastes based stochastic microsensors. RSC Adv. 2015;5:66185–91.
17. Gugoasa LA, Muklive Al'Ogaidi AJ, Stefan-van Staden RI, El-Khatib A, Rosu MC, Pruneanu S. Multimode microsensors based on Ag–TiO2–graphene materials used for the molecular recognition of carcinoembryonic antigen in whole blood samples. RSC Adv. 2017;7:28419–26.

18. Gugoasa LA, Muklive Al'Ogaidi AJ, Stefan-van Staden RI, Stanciu-Gavan C, van Staden JF, Rosu MC, et al. Molecular recognition of colon cancer biomarkers: P53, KRAS and CEA in whole blood samples. J Electrochem Soc. 2017;164:B443–7.
19. Stefan-van Staden RI, Balahura LR, Gugoasa LA, Aboul-Enein H, van Staden JF, Rosu MC, et al. Pattern recognition of 8-hydroxy-2′-deoxyguanosine in biological fluids. Anal Bioanal Chem. 2018;410:115–21.
20. Merchant CA, Healy K, Wanunu M, Ray V, Peterman N, Bartel J, et al. DNA translocation through graphene nanopores. Nano Lett. 2010;10:2915–21.
21. Siwy ZS, Davenport M. Nanopores: graphene opens up to DNA. Nat Nanotechnol. 2010;5:697–8.
22. Stargardt JF, Hawkridge FM, Landrum HL. Reversible heterogeneous reduction and oxidation of sperm whale myoglobin at a surface modified gold minigrid electrode. Anal Chem. 1978;50:930–2.
23. Pogacean F, Coros M, Magerusan L, Mirel V, Turza A, Katona G, et al. Exfoliation of graphite rods via pulses of current for graphene synthesis: sensitive detection of 8-hydroxy-2′-deoxyguanosine. Talanta. 2019;196:182–90.
24. Udayabhaskar R, Mangalaraja RV, Pandiyarajan T, Karthikeyan B, Mansilla HD, Contreras D. Spectroscopic investigation on graphene-copper nanocomposites with strong UV emission and high catalytic activity. Carbon. 2017;124:256–62.
25. Garaj S, Liu S, Golovchenko JA, Branton D. Molecule-hugging graphene nanopores. Proc Natl Acad Sci U S A. 2013;110:12192–6.
26. Hoogerheide DP, Gurnev PA, Rostovtseva TK, Bezrukov SM. Real-time nanopore-based recognition of protein translocation success. Biophys J. 2018;114:772–6.
27. Alotaibi MF. Physiology of puberty in boys and girls and pathological disorders affecting its onset. J Adolesc. 2019;71:63–71.
28. Loomba-Albrecht LA, Styne DM. The physiology of puberty and its disorders. Pediatr Ann. 2012;41:e1–9.
29. Qu Y, Berghman LR, Vandesande F. An electrochemical enzyme immunoassay for chicken luteinizing hormone: extension of the detection limit by adequate control of the nonspecific adsorption. Anal Biochem. 1998;259:167–75.
30. Pritchard DJ, Morgan H, Cooper JM. Simultaneous determination of follicle stimulating hormone and luteinising hormone using a multianalyte immunosensor. Anal Chim Acta. 1995;310:251–6.
31. Trevino J, Calle A, Rodriguez-Frade JM, Mellado M, Lechuga LM. Surface plasmon resonance immunoassay analysis of pituitary hormones in urine and serum samples. Clin Chim Acta. 2009;403:56–62.
32. Brindle E, Miller RC, Shofer JB, Klein NA, Soules MR, O'Connor KA. Urinary beta-luteinizing hormone and beta-follicle stimulating hormone immunoenzymometric assays for population research. Clin Biochem. 2006;39:1071–9.
33. Aizen J, Kasuto H, Levavi-Sivan B. Development of specific enzyme-linked immunosorbent assay for determining LH and FSH levels in tilapia, using recombinant gonadotropins. Gen Comp Endocrinol. 2007;153:323–32.